**Mutagenesis** vol. 29 no. 6 pp. 409–417
Advance Access publication 22 September 2014
doi:10.1093/mutage/geu049

# Correlation between *CYP1A1* transcript, protein level, enzyme activity and DNA adduct formation in normal human mammary epithelial cell strains exposed to benzo[a]pyrene

**Rao L. Divi, Tracey L. Einem Lindeman, Marie E. Shockley, Channa Keshava[1], Ainsley Weston[2] and Miriam C. Poirier***

Carcinogen-DNA Interactions Section, Center for Cancer Research, National Cancer Institute, National Institutes of Health, Bethesda, MD 20817, USA, [1]National Center for Environmental Assessment, Office of Research and Development, U.S. Environmental Protection Agency, Research Triangle Park, NC 27711, USA and [2]Division of Respiratory Disease Studies, National Institute for Occupational Safety and Health, Centers for Disease Control and Prevention, Morgantown, WV 26505, USA.

*To whom correspondence should be addressed. Tel: +301-402-1835; Fax: +301-402-8230; Email: poirierm@exchange.nih.gov

*Received on July 23, 2014; revised on August 18, 2014; accepted on August 19, 2014*

**The polycyclic aromatic hydrocarbon (PAH) benzo(a)pyrene (BP) is thought to bind covalently to DNA, through metabolism by cytochrome P450 1A1 (CYP1A1) and CYP1B1, and other enzymes, to form r7, t8, t9-trihydroxy-c-10-($N^2$-deoxyguanosyl)-7,8,9,10-tetrahydro-benzo[*a*]-pyrene (BPdG). Evaluation of RNA expression data, to understand the contribution of different metabolic enzymes to BPdG formation, is typically presented as fold-change observed upon BP exposure, leaving the actual number of RNA transcripts unknown. Here, we have quantified RNA copies/ng cDNA (RNA cpn) for *CYP1A1* and *CYP1B1*, as well as *NAD(P)H:quinone oxidoreductase 1* (*NQO1*), which may reduce formation of BPdG adducts, using primary normal human mammary epithelial cell (NHMEC) strains, and the MCF-7 breast cancer cell line. In unexposed NHMECs, basal RNA cpn values were 58–836 for *CYP1A1*, 336–5587 for *CYP1B1* and 5943–40 112 for *NQO1*. In cells exposed to 4.0 µM BP for 12 h, RNA cpn values were 251–13 234 for *CYP1A1*, 4133–57 078 for *CYP1B1* and 4456–55 887 for *NQO1*. There were 3.5 (mean, range 0.2–15.8) BPdG adducts/$10^8$ nucleotides in the NHMECs ($n$ = 16), and 790 in the MCF-7s. In the NHMECs, BP-induced *CYP1A1* RNA cpn was highly associated with BPdG ($P$ = 0.002), but *CYP1B1* and *NQO1* were not. Western blots of four NHMEC strains, chosen for different levels of BPdG adducts, showed a linear correlation between BPdG and CYP1A1, but not CYP1B1 or NQO1. Ethoxyresorufin-O-deethylase (EROD) activity, which measures CYP1A1 and CYP1B1 together, correlated with BPdG, but NQO1 activity did not. Despite more numerous levels of *CYP1B1* and *NQO1* RNA cpn in unexposed and BP-exposed NHMECs and MCF-7cells, BPdG formation was only correlated with induction of *CYP1A1* RNA cpn. The higher level of BPdG in MCF-7 cells, compared to NHMECs, may have been due to a much increased induction of CYP1A1 and EROD. Overall, BPdG correlation was observed with CYP1A1 protein and CYP1A1/1B1 enzyme activity, but not with CYP1B1 or NQO1 protein, or NQO1 enzyme activity.**

## Introduction

Polycyclic aromatic hydrocarbons (PAHs), partial combustion products of organic material, are ubiquitous in the environment (1), with human exposures coming primarily through inhalation and dietary routes (2). PAHs are human and animal carcinogens, and over the years animal models have provided critical insights into PAH carcinogenic mechanisms (3–5). For example, comparative dose/tumorigenicity studies of dibenzo[*a,l*]pyrene, 7,12-dimethyl-benz[*a*]anthracene, benzo[*a*]pyrene (BP) and two dibenzo[*a,l*]pyrene dihydrodiols have shown strong associations between dose level and tumour incidence in mice and rats (6). Similarly long-term studies using multiple levels of dosing have shown correlations between PAH–DNA adduct formation and tumorigenesis in trout (7) and mice (8,9). Epidemiologic studies, focused on relationships between PAH exposures, PAH–DNA adduct formation and cancer incidence (10), have shown increased risk of colon adenocarcinoma (11), and lung cancer (12) in individuals with the highest PAH–DNA adduct levels. Weak associations between exposure to PAHs and breast cancer have been reported in adults and post-menopausal women subjected to significant PAH exposures during early life (13–17).

PAHs, including BP, are activated to DNA binding species by cytochrome P450s (CYPs) and epoxide hydrolases (1,4,18). CYP1A1 and CYP1B1 are involved in the initial metabolic activation of PAHs, and CYP1B1 was 10-fold more active, compared to CYP1A1, in converting BP to the BP-7,8-diol (19). In addition to the CYPs, BP metabolism is impacted by the aldo-keto reductases (20), the glutathione transferases and NAD(P)H:quinone oxidoreductase 1 (NQO1). NQO1 was reported to exert a protective effect, reducing the level of PAH–DNA binding (21) and mutagenesis (22). In addition to the metabolic processes involving CYP1A1, CYP1B1 and NQO1, steady state levels of PAH–DNA adducts, often referred to as the biologically effective dose, are impacted by other metabolic enzymes (epoxide hydrolase, glutathione transferases), apoptosis, cell proliferation, DNA repair and peroxidase-mediated radical cation formation.

Previously, our studies employing microarrays and relative real-time PCR to measure fold-changes in gene expression, revealed up-regulation of *CYP1A1*, *CYP1B1* and *NQO1* expression in primary normal human mammary epithelial cells (NHMECs) exposed to BP (23). In addition, when a series of NHMEC strains were exposed to 4.0 µM BP for 12 h, the fold-inductions for both *CYP1A1* and *CYP1B1* expression weakly correlated with BPdG adducts formed in these cell strains (24). Whereas monitoring fold-changes in gene expression, in response to exposure, is excellent for screening purposes, pre-existing variations in basal levels of gene expression are not measured and are therefore overlooked. Here we have evaluated the actual numbers of gene transcripts, both before and after 12 h of exposure to BP, for *CYP1A1*, *CYP1B1* and *NQO1,* in NHMEC strains from 16 women, and the results represent

human interindividual variability on a small scale. We compared the gene transcript levels with BPdG levels, which were measured in the same cell strains and reported previously (24). Finally, in a subset of four of these NHMEC strains, chosen for their different levels of BPdG formation, we evaluated protein levels of CYP1A1, CYP1B1 and NQO1 by western blot, and enzyme activities. Ethoxyresorufin-O-deethylase (EROD) assay, was used to measure CYP1A1 and CYP1B1 activities together, and NQO1 activity was also measured by enzyme assay. The BPdG values were then compared to the RNA cpn, protein levels and enzyme activities.

## Materials and methods

*Cell culture and chemicals*

NHMECs were isolated from normal breast tissue, and collected at reduction mammoplasty by a process involving mechanical and enzymatic disruption (25). The tissue was obtained through the Cooperative Human Tissue Network, which is sponsored by the National Cancer Institute and the National Disease Research Interchange. Human Studies Review Board approval was sought at the National Institute for Occupational Safety and Health, where the tissue was received and the cells were derived, and a waiver was granted because no unique identifiers accompanied the tissues. Uniform cultures of epithelial cells were obtained by growing enzyme disrupted cells for six passages in serum free mammary epithelial growth medium (MEGM) (Clonetics™, Walkersville, MD). MCF-7 cells, purchased from the American Type Culture Collection (ATCC, Manassas, VA) were grown in minimal essential medium containing 2 mM L-glutamate (Clonetics™) and 10% fetal bovine serum.BP (99% purity) was purchased from the National Cancer Institute Chemical Carcinogen Reference Standard Repository, Midwest Research Institute (Kansas City, MO).

*Exposure of NHMECs and MCF-7 cells to BP, cell survival and DNA preparation*

For these experiments semi-confluent NHMEC strains from 16 different individuals, and MCF-7 cells, were exposed to 4.0 µM BP for 12 h (23,24). Cell survival, examined by Cell Titer-Glo Luminescent Assay (Promega, Madison, WI) in the MCF-7 cells and in four of the NHMEC strains, was ≥87%. For the complete set of 16 NHMEC strains, and the MCF-7 cells, BP exposures were performed twice, and RNA transcript analysis and BPdG analyses were performed three times on each sample.

For DNA preparation, cells were washed with PBS, lysed with 5 ml lysis buffer (Qiagen, Valencia, CA) and incubated with RNase A (250 µg, Qiagen) for 20 min at 37°C followed by proteinase K (500 µg, Qiagen) for 3 h at 50°C. At the end of the proteinase K digestion, an equal volume of 100% ethanol was added to each sample and the DNA was isolated using Qiagen columns. The DNA was eluted in molecular biology grade water (26), and stored at −70°C. The quality and quantity of the DNA was measured by UV spectrophotometry at 260/280 nm, and then DNA was reconstituted to the required concentrations using TE buffer (pH 7.4, 1×).

*Preparation of RNA and cDNA synthesis*

Total RNA was isolated from cells using the RNeasy kit (Qiagen), as per the manufacturer's protocol. RNA was resuspended in 50 µl of nuclease-free water, and the concentration was measured by spectrophotometry, while the purity and quality were measured by gel electrophoresis. RNA (12 µg) was converted to cDNA using the qPCR kit by Affymetrix (Affymetrix, Santa Clara, CA) with oligonucleotide $(dT)_{24}$ primers. Unused nucleotides and primers were removed from cDNA by column filtration (Microcon YM-30, Millipore, Billerica, MA) and quantity of cDNA was measured by fluorescence spectroscopy using SYBR green at excitation and emission wavelengths of 492 and 526 nm, respectively.

*CYP1A1, CYP1B1 and NQO1 RNA cpn by quantitative real-time PCR*

Quantitation of RNA cpn was accomplished by quantitative real-time PCR (qRT-PCR) using gene specific primers and SYBR green (Bio-Rad, Hercules, CA, USA). qRT-PCR was performed in a total volume of 25 µl reaction mixture containing 1× iQ SYBR Green Supermix, 333 nM gene specific primers and an aliquot of cDNA. A standard curve was generated using human universal cDNA (Clontech, Mountain View, CA, USA). A three-step PCR reaction was performed using the iQ5 real-time PCR detection system (Bio-Rad). Universal cDNA having 46 000, 133 000 and 25 000 copies of *CYP1A1, CYP1B1* and *NQO1* per microgram of cDNA, respectively, was serially diluted to have 0–5712 copies of *CYP1A1*, 0–16 608 copies of *CYP1B1* and 0–3120 copies of *NQO1* per reaction vial, and mixed with iQ SYBR Green Supermix (1×) and 330 nM gene specific primers (*CYP1A1*: forward primer 5′-CACCTCCAAGATCCCTACACTGA-3′ and reverse primer 5′-ACCAGACAGAAGATGACAGAGGC-3′; *CYP 1B1*: forward primer 5′-ATGTCCTGGCCTTCCTTTATGA-3′ and reverse primer 5′- AGACAGAGGTGTTGGCAGTG-3′; and *NQO1*: forward primer 5′-ATGGTCGGCAGAAGAGCACT-3′ and reverse primer 5′-ACCACCTCCCA-TCCTTTCTT-3′) for real-time PCR amplification to obtain cycle threshold ($C_T$) values. The copy numbers in the universal cDNA were established using varying concentrations of genomic DNA as standard, assuming that one human somatic cell contains 7.12 pg of genomic DNA and two copies of each gene, and the $C_T$ values determined for the genomic DNA. Each NHMEC/MCF-7 cDNA sample was assayed in duplicate and the copy numbers were determined using the universal cDNA standard curve and expressed as RNA cpn.

*Quantification of BPdG adducts*

The r7, t8-dihydroxy-t-9,10-epoxy-7, 8, 9, 10-tetrahydrobenzo[*a*]pyrene (BPDE)–DNA chemiluminescence immunoassay (CIA) was performed as described (27) with minor modifications. The BPdG values presented here for NHMECs were previously generated in this laboratory from duplicate experiments and reported (24). For the current studies, the previously reported BPDE–DNA CIA values were used, but the same NHMEC strains were grown again and assayed for RNA cpn. In addition, the MCF-7 cells were exposed to 4 µM BPDE for 12 h, the DNA was extracted and assayed by BPDE–DNA CIA. The lower limit of detection of the BPDE–DNA CIA, using 10 µg DNA, was 0.3 adducts/$10^8$ nucleotides. The BPDE–DNA standard curve in the CIA showed 50% inhibition at 0.60 ± 0.08 fmol BPdG (mean ± SE, $n$ = 30).

*CYP1A1 and 1B1 protein levels determined by western blot*

Western blotting was employed to evaluate CYP1A1, CYP1B1 and NQO1 protein levels in four NHMEC strains, M98030, M99016, M000012 and M98026, which had BPdG levels of 2.6, 4.1, 5.9 and 10.6 adducts/$10^8$ nucleotides, respectively. Proteins from cell lysates were separated by sodium dodecyl sulfate-polyacrylamide gel electrophoresis, transferred to a nitrocellulose membrane (Applied Biosystems, Foster City, CA, USA), and probed with specific antibodies for CYP1A1 (GENTEST BD Biosciences, Woburn, MA, USA), CYP1B1 (GENTEST BD Biosciences), NQO1 (Novus Biologicals, Littleton, CO, USA) and β-actin (Chemicon International, Atlanta, GA, USA). The protein bands were visualised after incubation with secondary antibody conjugated to streptavidin-alkaline phosphatase followed by Nitro-Block Enhancer (Applied Biosystems, Bedford, MA, USA) and CDP-Star (Applied Biosystems). Blots were repeated 4–6 times.

*CYP1A1 and 1B1 activity determined by EROD assay*

EROD assays were conducted on cells cultured to semi-confluence in 12-well plates with 1 ml medium/well and exposed to 4.0 µM BP for 12 h. After incubation, the medium was removed and the wells were washed three times with Dulbecco's phosphate buffered saline (DPBS). EROD activity was measured as previously described (28,29) with slight modifications. Intact cells were incubated in 250 µl of DPBS containing 5 µM ethoxyresorufin and 1.5 mM salicylamide for 20 min at 37°C. At the end of incubation, duplicate aliquots of 100 µl were transferred to wells of an opaque 96-well plate. The resorufin formed was measured using an Infinite 200 fluorescence reader (Teacan, Männedorf, Switzerland) set at excitation and emission wavelengths of 560 and 592 nm, respectively. Values (fmol/min/mg protein) for exposure groups were calculated using a resorufin standard curve generated using the same 96-well plates. After completion of the EROD assay, the wells were washed with PBS, lysed in 250 µl of PBS using sonicator set 20% amplitude in a five 4 s pulses with 5 s of interval to prevent increase of temperature in the wells. An aliquot of the lysate was transferred to polypropylene 96-well plate (Grainer Bio) and used for measuring protein by Pierce Bicinchoninic Acid protein assay as per the manufacturers' protocol (Thermo Scientific, Rockford, IL) using BSA as standard.

*NQO1 activity by enzyme assay*

Spectrophotometric analysis (30) of NQO1 was followed at 600 nm, using 40 µM 2,6-dicholoroindophenol as substrate, 200 µM NADH with or without 20 µM dicumerol. Activity was expressed as the dicumerol-sensitive decrease in absorbance or µmoles 2,6-dicholo-indophenol reduced/min/mg protein. Protein was measured by Pierce Bicinchoninic Acid protein assay (Thermo Scientific).

*Statistical analysis*

The statistical significance of the resulting changes was analysed using SigmaStat 3.11 (Systat Software, Inc., San Jose, CA). The BP-exposed cells were compared to the unexposed controls, and when the equality of the

variance and the normality of the data were confirmed, they were further analysed by *t*-test. Correlations between BPdG adduct level and *CYP1A1*, *CYP1B1* and *NQO1* RNA cpn, or CYP1A1, CYP1B1 and NQO1 protein expression, or EROD and NQO1 enzyme assays, were determined using the Spearman test and/or the Pearson product moment correlation statistic with a correlation coefficient window of (−1) to (+1).

## Results

### *BPdG levels in the NHMEC strains and MCF-7 cells*

The 16 strains of NHMECs, and the MCF-7 cells, were exposed to 4.0 µM BP for 12 h and evaluated for BPdG by BPDE–DNA CIA. For the NHMECs, Table 1 shows variability for BPdG levels ranging from 0.2 to 15.8 BPdG adducts/$10^8$ nucleotides, with the median at 1.9 BPdG adducts/$10^8$ nucleotides. The BPdG values (Table 1) were reported previously (24). Table 1 also shows an adduct value of 790 BPdG adducts/$10^8$ nucleotides for MCF-7 cells, which was approximately 400-fold higher than the NHMEC values.

### *RNA cpn for CYP1A1, CYP1B1 and NQO1 in the NHMEC strains and MCF-7 cells*

For the genes of interest, RNA cpn values shown in Table 1 include the 16 NHMEC strains and the MCF-7 cells. The Table presents RNA cpn for unexposed cells (basal or endogenous levels), and BP-exposed cells (BP-induced levels). For *CYP1A1*, in unexposed NHMEC's, RNA cpn values ranged from 58 to 836, and in BP-exposed cells values ranged from 251 to 13 234. The individual fold-increase values for *CYP1A1* were between 3-fold and 78-fold. In addition, between the median basal value of 294 RNA cpn, and the median BP-induced value of 2859 RNA cpn, a 10-fold increase was observed for *CYP1A1*.

In contrast to *CYP1A1*, for *CYP1B1* the NHMEC basal RNA transcripts were more numerous, ranging from 336 to 5587 RNA cpn, with a median of 2503 for unexposed cells. In the BP-exposed cells the induced RNA cpn range was 4133–57 077, with a median of 20 432. For *CYP1B1,* fold inductions ranged from 3 to 60, with a median of 9.5. Whereas the fold-increases for BP induction of *CYP1A1* and *CYP1B1*, were in a similar range, Table 1 shows that the numbers of RNA transcripts for *CYP1B1* were substantially higher than those for *CYP1A1,* in the same cell strains.

Table 1 also gives RNA cpn values for *NQO1* in unexposed and BP-exposed NHMECs. In contrast to *CYP1A1* and *CYP1B1,* in some cell strains there was no *NQO*1 induction by BP, and in others the induction was minimal (<2-fold). The median RNA cpn values for unexposed and BP-exposed groups were 23 336 and 32 440, respectively. Substantial interindividual variability was displayed among NHMEC strains, with regard to change in *NQO1* RNA cpn level in response to BP exposure, as 13 strains showed a modest induction with BP, 2 strains showed a decrease with BP, and 1 did not change.

For MCF-7 cells, the *CYP1A1* RNA cpn was nine in unexposed cells and 3413 in BP-exposed cells, giving a 379-fold induction in the presence of BP. This was a much greater induction than that found in the NHMECs, and likely contributed to the high BPdG levels observed in these cells. For MCF-7 cells the *CYP1B1* RNA cpn was 1144 in unexposed cells and 33 792 in BP-exposed cells, giving a 29-fold induction in the presence of BP. This was similar to the induction observed in the NHMECs. For *NQO1* RNA cpn the MCF-7 cells showed a 1.6-fold modest induction in the BP-exposed cells compared with the unexposed cells. The substantial *CYP1A1* induction in BP-exposed MCF-7 cells suggested a rationale for the high BPdG level (790 adducts/$10^8$ nucleotides) observed with the same concentration of BP exposure, compared to NHMECs (mean 3.5 BPdG/$10^8$ nucleotides). With the exception of basal levels of *CYP1A1*, the RNA cpn values shown in Table 1 for the MCF-7 cells were within the range for those seen for the NHMECs.

### *Comparison of CYP1A1, CYP1B1 and NQO1 RNA cpn and BPdG adducts in the NHMEC strains*

A major goal in designing these studies was to evaluate correlations between BPdG adduct formation and

**Table I.** BPdG adducts/$10^8$ nucleotides [from ref. (24)] and RNA copies/ng cDNA[a] for *CYP1A1, CYP1B1* and *NQO1* in 16 strains of NHMECs, and MCF-7 cells, without and with 12 h of exposure to 4.0 µM BP

| NHMEC | BPdG/$10^8$ | *CYP1A1*[a] | *CYP1A1*[a] | *CYP1B1*[a] | *CYP1B1*[a] | *NQO1*[a] | *NQO1*[a] |
|---|---|---|---|---|---|---|---|
| Strain ID | Nucleotides | Unexposed | BP-exposed | Unexposed | BP-exposed | Unexposed | BP-exposed |
| M99004 | 15.8 | 586 | 9850 | 1436 | 33 293 | 16 489 | 27 469 |
| M99005 | 0.2[b] | 446 | 2352 | 4744 | 31 980 | 40 112 | 38 060 |
| M99006 | 1.8 | 308 | 1008 | 3222 | 12 450 | 20 935 | 30 467 |
| M99016 | 4.1 | 748 | 3799 | 2618 | 25 864 | 37 949 | 55 887 |
| M99021 | 1.0 | 291 | 1022 | 2388 | 7487 | 25 017 | 31 395 |
| M99025 | 0.9 | 164 | 793 | 1763 | 20 608 | 39 600 | 34 696 |
| M00012 | 5.9 | 578 | 7609 | 1020 | 13 298 | 15 820 | 19 034 |
| M98019 | 3.1 | 90 | 251 | 2988 | 8489 | 20 967 | 22 734 |
| M98025 | 0.2[b] | 175 | 7166 | 1379 | 22 366 | 34 023 | 34 326 |
| M98026 | 10.6 | 169 | 13 234 | 661 | 39 433 | 19 110 | 33 729 |
| M98035 | 1.2 | 58 | 285 | 3806 | 17 864 | 23 704 | 31 356 |
| M98030 | 2.6 | 150 | 2532 | 4599 | 57 078 | 29 612 | 36 482 |
| M99003 | 1.3 | 392 | 3186 | 4645 | 43 642 | 29 302 | 33 484 |
| M98021 | 0.9 | 836 | 3408 | 5587 | 20 255 | 18 651 | 25 583 |
| M98011 | 2.0 | 296 | 6511 | 1218 | 10 365 | 20 695 | 35 029 |
| M00015 | 4.3 | 103 | 1391 | 336 | 4133 | 5943 | 4456 |
| Mean ($n$ = 16) | 3.5 | 337 | 4025 | 2651 | 23 038 | 24 871 | 30 887 |
| *P value* | | | | | | | |
| BPdG vs RNA cpn | | 0.488 | 0.002 | 0.059 | 0.404 | 0.079 | 0.572 |
| MCF-7 | 790.0 | 8.8 | 3412.7 | 1143.7 | 33 792.3 | 9158.3 | 14 521.4 |

[a]RNA cpn.
[b]These samples were non-detectable and for the purposes of the calculations they were given values of 0.15 (rounded to 0.2), half way between the limit of detection (0.3 BPdG/$10^8$ nucleotides) and 0.

expression levels of metabolic enzymes responsible for BP biotransformation. In Figure 1 we present data for the relationship between BPdG levels and RNA cpn, where the basal or endogenous RNA cpn values were subtracted from the induced cpn values, and plotted as a function of BPdG level. There was a highly-significant relationship between BPdG levels and *CYP1A1* RNA cpn for the 16 NHMEC strains (Figure 1A), indicating that BP-induced CYP1A1 levels were strongly positively-associated with BPdG formation ($P = 0.002$). In contrast, in the same NHMEC strains, induced levels of *CYP1B1* RNA cpn (Figure 1B) were not significantly associated with BPdG formation ($P = 0.278$), suggesting a more complicated relationship between this enzyme and BPdG formation in NHMECs. By comparing the RNA cpn values for *CYP1A1* and *CYP1B1* in Figure 1A and B, respectively (also Table 1), it is apparent that the BP-induced *CYP1B1* RNA cpn levels were about 4-fold higher than those for *CYP1A1*. Finally, Figure 1C shows a similar graph for *NQO1*, in which there was no correlation between BP-induced *NQO1* RNA cpn and BPdG adduct formation (Pearson $P = 0.109$; Spearman $P = 0.06$). Although Figure 1 shows BPdG plotted as a function of RNA cpn where the basal levels of RNA cpn have been subtracted, the graphs of the original data showed the same relationships (data not shown).

### *Western blots for CYP1A1, CYP1B1 and NQO1 in four NHMEC strains*

Using four NHMEC strains chosen to span the spectrum of BPdG levels from high to low ($n = 4$), Western blots were performed to evaluate protein levels for CYP1A1, CYP1B1 and NQO1. Figure 2 shows representative western blots for CYP1A1 in unexposed cells (A) and BP-exposed cells (B) and quantitative (C) CYP1A1 western blot data ($n \geq 4$), expressed as a function of β-actin levels. Figure 2D, similar to Figure 1A, shows a strong positive correlation between CYP1A1 protein level and formation of BPdG adducts in the four chosen cell strains ($P = 0.0128$).

Using the same four NHMEC strains we examined protein levels of CYP1B1 by western blot and the results are shown in Figure 2. Again, representative blots for unexposed cells (Figure 2E) and BP-exposed cells (Figure 2F) are shown, as well as CYP1B1 protein quantitation for ≥4 western blots (Figure 2G). Finally, Figure 2H shows the lack of a correlation between BP-induced levels of CYP1B1 protein and BPdG adducts in the four cell strains ($P = 0.696$).

Similarly, we examined protein levels of NQO1 by western blot and the results are shown in Figure 2. Again, representative blots for NQO1 in unexposed cells (Figure 2I) and BP-exposed cells (Figure 2J) are shown, as well as protein level quantitation for ≥4 western blots (Figure 2K). Figure 2L shows the lack of a correlation between BP-induced levels of NQO1 and BPdG adducts ($P = 0.874$).

By western blots, in addition to the four strains of NHMECs, we also examined MCF-7 cells. For CYP1A1 (Figure 2C) and for NQO1 (Figure 2K) BP exposure caused large inductions of the enzyme protein levels, but there was no induction of CYP1B1 (Figure 2G).

### *EROD enzyme activity and NQO1 enzyme activity in four NHMEC strains*

Confirmation of the above mentioned relationships was obtained by measurement of enzyme activities in the same four NHMEC strains. Combined CYP1A1/1B1 activity was measured by EROD assay (Figure 3), and NQO1 activity was measured by a dicumerol-sensitive assay (Figure 4).

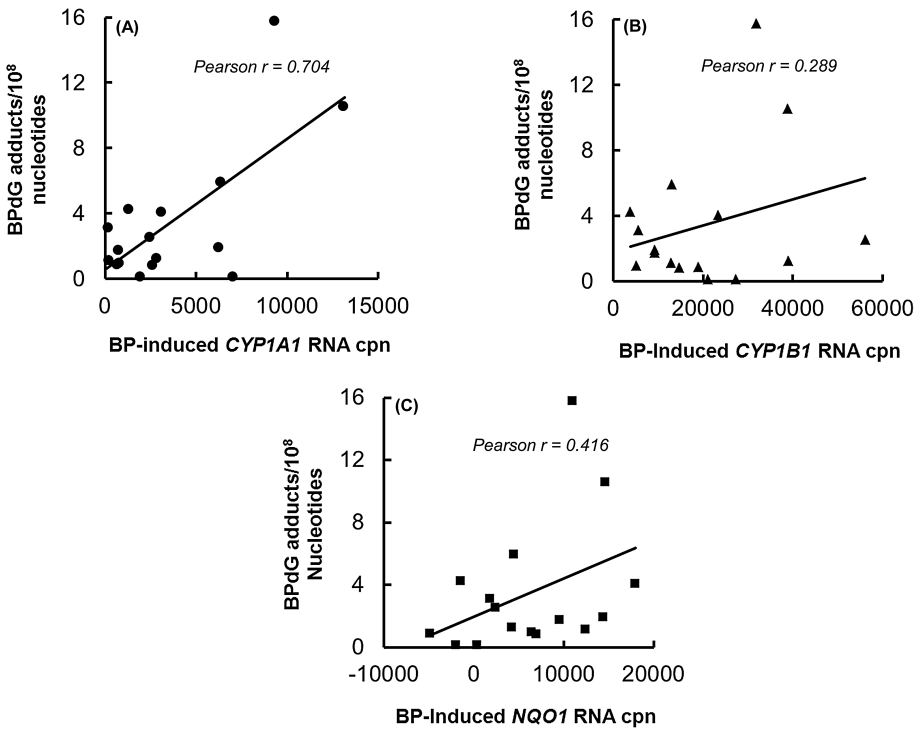


**Fig. 1.** Correlation between BPdG adduct formation and BP-induced RNA cpn for *CYP1A1* (**A**), *CYP1B1* (**B**), and *NQO1* (**C**), in 16 strains of NHMECs, where the corresponding basal or endogenous levels of RNA cpn have been subtracted. By Pearson and/or Spearman rank correlation statistical analysis: (A) Pearson $P = 0.002$; (B) Pearson $P = 0.278$; (C) Pearson $P = 0.109$ and Spearman $P = 0.06$.

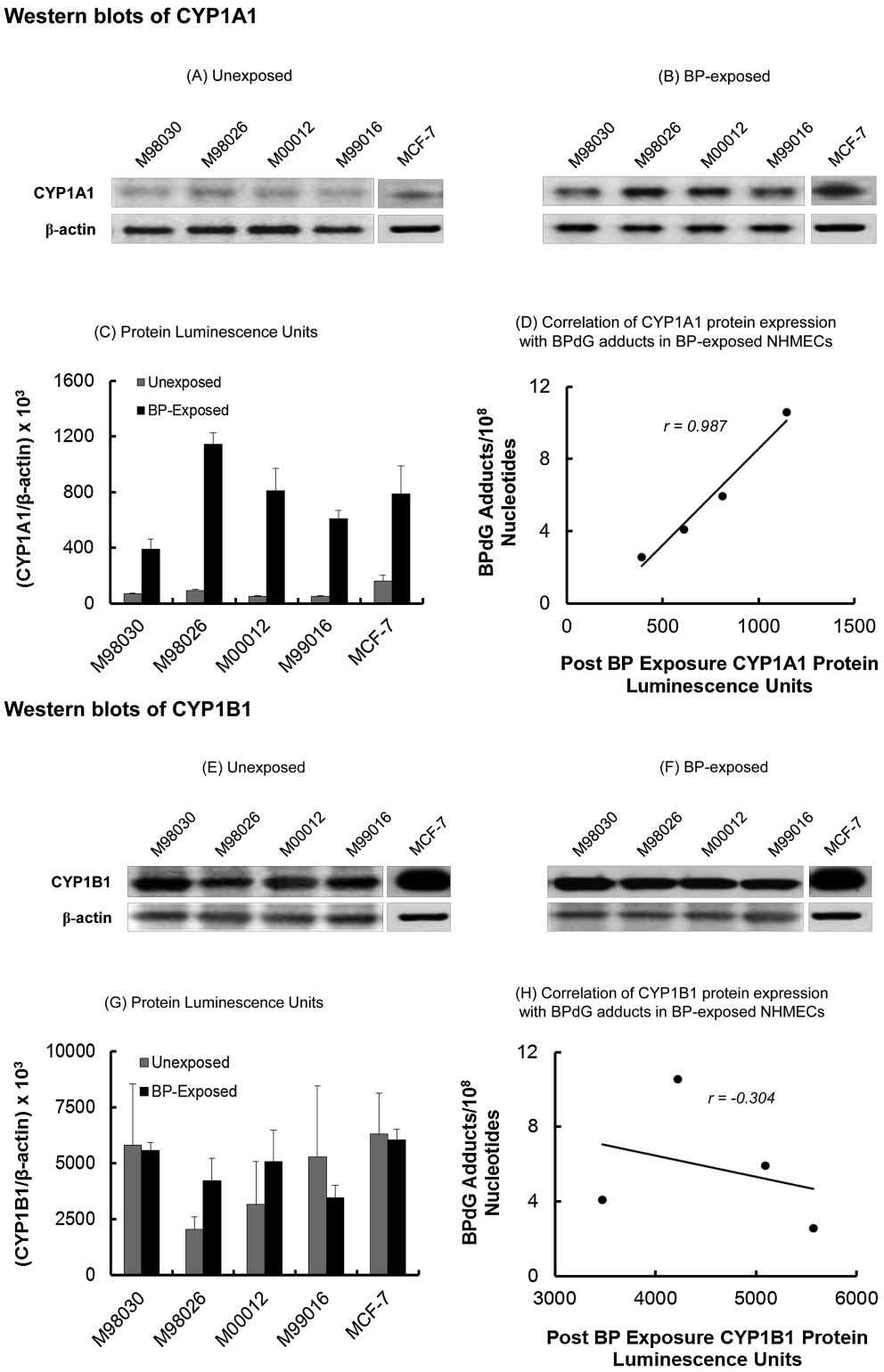


Figure 3A shows EROD activity for the four NHMEC strains and MCF-7 cells, and Figure 3B shows a strong correlation between BPdG adduct formation and EROD activity, which is presumably driven by CYP1A1 ($P$ = 0.038). Note that the induced EROD activity in the MCF-7 cells is much higher than that in the NHMECs (Figure 3A), suggesting that this may contribute to the high BPdG levels seen in the MCF-7 cells.

Figure 4A shows NQO1 activity in the NHMECs and MCF-7 cells, indicating that BP-induction of this enzyme is lacking in some cell strains. In the MCF-7 cells, levels of NQO1 activity were similar to those observed in the NHMECs. Figure 4B shows that there may be an inverse correlation between BPdG formation and BP-induced NQO1 enzyme activity ($r$ = −0.524) but the association was lacking statistical significance.

## Discussion

In this study, we have used NHMEC strains, which are not cell lines but are primary cells cultured from healthy normal breast tissue obtained at reduction mammoplasty, to evaluate

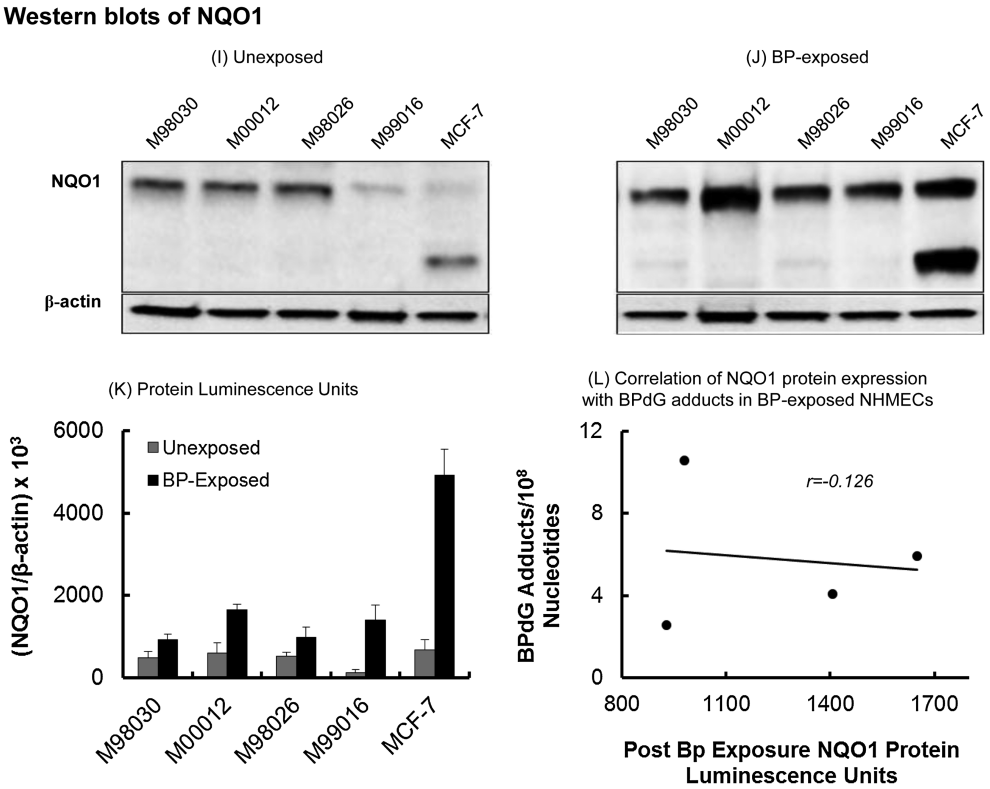


**Fig. 2.** Western blot analyses for CYP1A1 (**A**–**D**), CYP1B1 (**E**–**H**) and NQO1 (**I**–**L**) for four NHMEC strains having different levels of BPdG, as well as MCF-7 cells. These are M98030, M99016, M00012 and M98026 having 2.6, 4.1, 5.9 and 10.6 BPdG adducts/$10^8$ nucleotides, respectively. A, E and I show representative blots for unexposed cells; B, F and J show representative blots for exposed cells; C, G and K show protein levels (mean ± SD in luminescence units) for ≥4 western blots per protein; D, H and L show the correlation between NHMEC protein level and BPdG adducts, where statistical significance ($P = 0.0128$) was observed only with D.

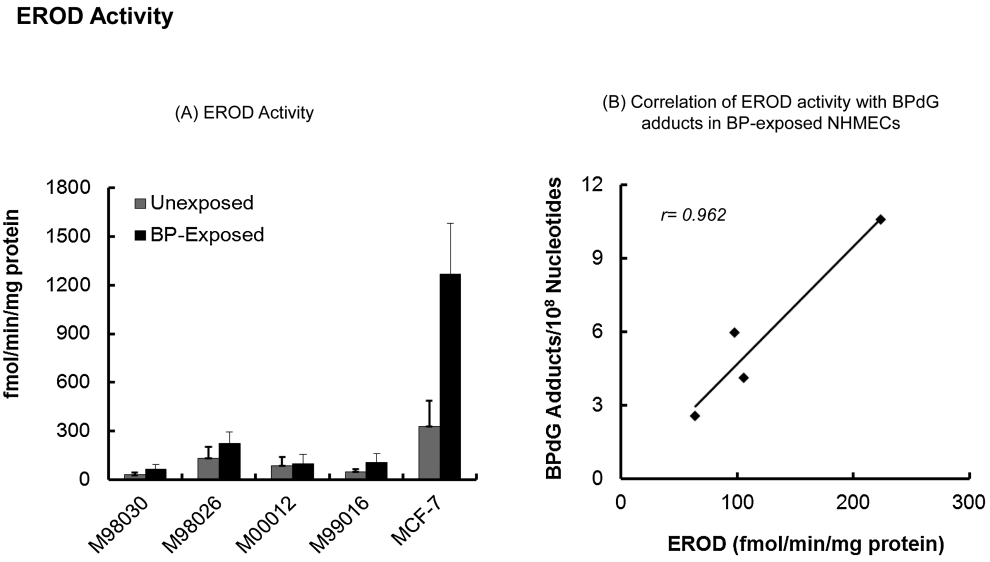


**Fig. 3.** EROD enzyme activity, comprising both CYP1A1 and CYP1B1 activities, for (**A**) unexposed (□) and BP-exposed (■) NHMECs ($n = 4$ strains; see legend to Figure 2) and MCF-7 cells; (**B**) comparison between BPdG adduct formation and EROD activity ($P = 0.038$) in NHMECs.

interindividual variability in BP bio-transformation and DNA adduct formation. Comparison of RNA cpn with BPdG adduct level was achieved for *CYP1A1*, *CYP1B1* and *NQO1* in the 16 NHMEC strains. Further evaluation of CYP1A1, CYP1B1 and NQO1 proteins by western blot, and enzyme activities by EROD and NQO1 assays was carried out in four NHMEC strains chosen because they had varying levels of BPdG adduct, from high to low. Overall the study shows that, of the three enzymes studied, CYP1A1 induction is the driving force behind BPdG formation in NHMECs. Significant correlations were found between BPdG adduct level and *CYP1A1* RNA cpn, CYP1A1 protein level by western blot, and EROD activity, presumably through CYP1A1, though the assay also measures CYP1B1. The study also shows that *CYP1B1* RNA transcripts, in both unexposed and exposed cells, are much more abundant than *CYP1A1* RNA transcripts, despite the fact that they do not

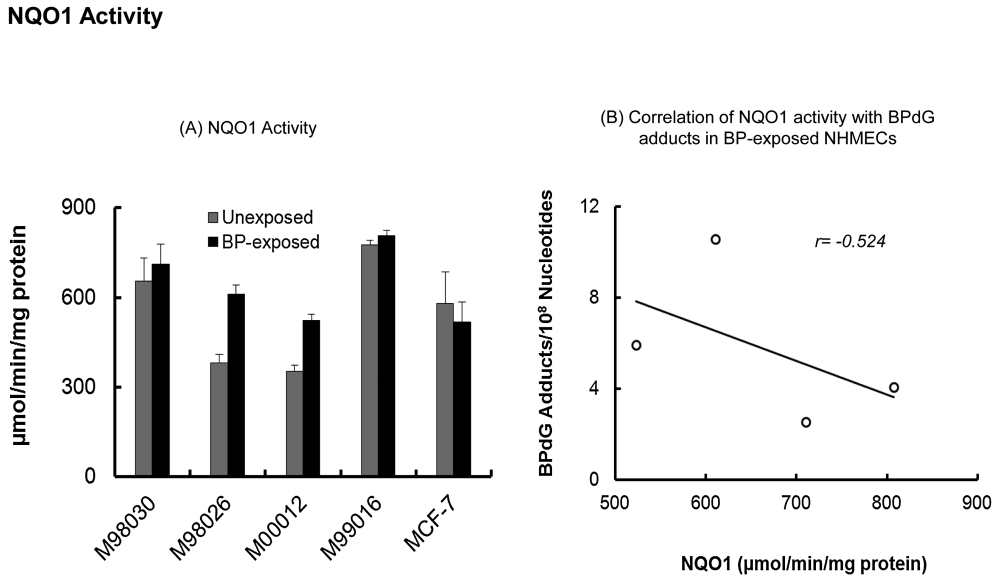


**Fig. 4.** NQO1 enzyme activity for (**A**) unexposed (□) and BP-exposed (■) NHMECs ($n = 4$ strains; see legend to Figure 2) and MCF-7 cells; (**B**) the comparison between BPdG adduct formation and NQO1 activity in NHMECs was not significant.

correlate with BPdG formation. *NQO1* RNA transcripts are not consistently induced by BP in the NHMECs and therefore there was no correlation, either positive or negative, with BPdG formation.

The data presented here show a novel evaluation of RNA expression for *CYP1A1*, *CYP1B1* and *NQO1*. The power of this approach, a quantitation of RNA transcript copies before and after induction by chemical exposure, is the capacity to reveal endogenous and xenobiotic-induced levels of RNA transcripts as specific numbers, rather than the usual fold-change documented by microarray or RT-PCR. In the NHMECs we observed that endogenous or basal levels of *CYP1A1* are several-fold lower than endogenous levels of *CYP1B1*, despite the greater magnitude of BP-associated induction typically seen with *CYP1A1*. This complicates the role of CYP1B1 in BPdG formation in NHMECs. Table 1 shows that endogenous levels of *CYP1B1* were associated with BPdG levels ($P = 0.031$ by Spearman rank correlation), suggesting that this enzyme may play a subtle role in modulating the low levels of BP/PAH exposures that are chronically prevalent in our environment. Reports in the literature have shown CYP1B1 to have both activating and protective effects, and the ultimate role for this enzyme appears to vary with cell type, organ and whole animal (31).

In these studies MCF-7 breast cancer cells were given the same BP exposure conditions as the NHMECs, and the BPdG adduct levels were more than 400-fold higher than those found in the NHMECs. Interestingly, the magnitude of this difference is not completely explicable by differences in RNA cpn for the enzymes evaluated here, as the BP-induced levels for *CYP1A1*, *CYP1B1* and *NQO1* in MCF-7 cells were within values generated for the BP-exposed NHMECs. However, the EROD activity levels in BP-exposed MCF-7 cells, in the range of 1200 fmol/min/mg protein, were much higher than those observed in the NHMECs, which averaged 125 fmol/min/mg protein, suggesting that EROD activity may be an important contributing factor. Interestingly, BP-exposed MCF-7 cells had high levels of NQO1 protein by western blot, but the NQO1 enzyme activity was not induced by BP in these cells. The use of MCF-7 cells alone provides limited information, since they are abnormal and represent only one phenotype, however, the comparison with the NHMECs does provide an interesting contrast. Overall the data suggest that the expressed enzyme levels contribute more to BPdG adduct formation than the numbers of RNA cpn, which were similar in both NHMECs and MCF-7 cells.

These studies were performed using 16 different strains of normal human breast epithelial cells, all obtained from different individuals. The variability observed here provides an indication of human interindividual variability for formation of BPdG adducts. Considering the ubiquitous nature of PAH exposures, and indications that PAH–DNA adducts form in many organs of the human body (32), it is interesting to find only a 15-fold difference in BPdG level across these 16 NHMEC strains. There are many studies in the literature documenting PAH exposures and PAH–DNA adduct formation in the human population, and in some organs PAH–DNA adduct formation indicates both exposure and cancer risk (10,32). However, an association between PAH–DNA adduct formation and an increase in breast cancer risk is not always found, and is at best a weak one (13,14,16,33). Neither the early studies summarised in (34), nor the more recent larger trials, supported an association between increased risk of breast cancer and high levels of bulky DNA adducts measured by $^{32}$P-postlabelling (17,35), or high levels of PAH–DNA adducts measured by BPDE–DNA ELISA. Therefore, the results of this study may tell us more about human interindividual variability with respect to PAH exposure, than human breast cancer risk.

A wealth of published information suggests conflicting roles for BP metabolism by CYPs in different tissues or cells. In the mouse, BP or PAH induction of CYP1A1 was associated with dose-related DNA damage in target organs and tumour incidences (8,36). That paradigm was largely supported in the studies presented here. However, studies utilizing genetically modified mouse models have revealed a complex picture. For example, in *CYP1* knockout mice, inducible CYP1A1 was important for detoxification of reactive BP metabolites in intestine and liver, while CYP1B1 was responsible for metabolic activation of BP in spleen and bone marrow, causing immune damage in the absence of CYP1A1 (37). In the cytochrome P450 oxidoreductase null (HRN) mouse model, higher BPdG levels were observed in livers of HRN mice compared to livers

of wild type mice (38). Therefore, at least some of the CYP enzymes may have inhibited activation of BP to DNA binding species in the HRN mice. In a study using genetically modified mice with varying levels of the aryl hydrocarbon receptor (AhR), increased levels of BPdG adducts and BP metabolites were found in several organs of AhR null mice, compared to AhR (+/+) and AhR (+/−) mice, also suggesting that Ahr-independent pathways may contribute to BPdG formation in AhR null mice (39).

In conclusion, the data presented here show that, despite the much higher RNA levels of endogenous and BP-induced CYP1B1, there was no association between BPdG formation and BP-induced CYP1B1. *CYP1A1* RNA expression, CYP1A1 protein levels, and EROD (CYP1A1 plus CYP1B1) enzyme activity were all associated with BPdG adduct formation, suggesting that CYP1A1 is more important than CYP1B1 or NQO1 in the metabolic events governing the formation of BPdG in NHMECs. The data also suggest that individuals with the lowest levels of *CYP1A1* RNA cpn in breast may have the lowest PAH–DNA adduct levels, though it is not clear if this is a breast cancer-related risk factor.

## Funding

This research was supported by the intramural research program of the Center for Cancer Research, National Cancer Institute, National Institutes of Health, and the intramural Health Effects Laboratory Division of the National Institute for Occupational Safety and Health, Centers for Disease Control.

Conflict of interest statement: None declared.

## References

1. IARC. (2010) Some non-heterocyclic polycyclic aromatic hydrocarbons and some related exposures. *IARC Monogr. Ser*., **92**, 1–853.
2. Phillips, D. H. (1983) Fifty years of benzo(a)pyrene. *Nature*, **303**, 468–472.
3. Boutwell, R. K. (1989) Model systems for defining initiation, promotion, and progression of skin neoplasms. *Prog. Clin. Biol. Res*., **298**, 3–15.
4. Sims, P., Grover, P. L., Swaisland, A., Pal, K. and Hewer, A. (1974) Metabolic activation of benzo(a)pyrene proceeds by a diol-epoxide. *Nature*, **252**, 326–328.
5. Stenbäck, F., Peto, R. and Shubik, P. (1981) Initiation and promotion at different ages and doses in 2200 mice. III. Linear extrapolation from high doses may underestimate low-dose tumour risks. *Br. J. Cancer*, **44**, 24–34.
6. Cavalieri, E. L., Higginbotham, S., RamaKrishna, N. V., Devanesan, P. D., Todorovic, R., Rogan, E. G. and Salmasi, S. (1991) Comparative dose-response tumorigenicity studies of dibenzo[alpha,l]pyrene versus 7,12-dimethylbenz[alpha]anthracene, benzo[alpha]pyrene and two dibenzo[alpha,l]pyrene dihydrodiols in mouse skin and rat mammary gland. *Carcinogenesis*, **12**, 1939–1944.
7. Pratt, M. M., Reddy, A. P., Hendricks, J. D., Pereira, C., Kensler, T. W. and Bailey, G. S. (2007) The importance of carcinogen dose in chemoprevention studies: quantitative interrelationships between, dibenzo[a,l]pyrene dose, chlorophyllin dose, target organ DNA adduct biomarkers and final tumor outcome. *Carcinogenesis*, **28**, 611–624.
8. Culp, S. J., Warbritton, A. R., Smith, B. A., Li, E. E. and Beland, F. A. (2000) DNA adduct measurements, cell proliferation and tumor mutation induction in relation to tumor formation in B6C3F1 mice fed coal tar or benzo[a]pyrene. *Carcinogenesis*, **21**, 1433–1440.
9. Culp, S. J. and Beland, F. A. (1994) Comparison of DNA adduct formation in mice fed coal tar or benzo[a]pyrene. *Carcinogenesis*, **15**, 247–252.
10. Poirier, M. C. (2012) Chemical-induced DNA damage and human cancer risk. *Discov. Med*., **14**, 283–288.
11. Gunter, M. J., Divi, R. L., Kulldorff, M., *et al*. (2007) Leukocyte polycyclic aromatic hydrocarbon-DNA adduct formation and colorectal adenoma. *Carcinogenesis*, **28**, 1426–1429.
12. Tang, D. L., Rundle, A., Warburton, D., Santella, R. M., Tsai, W. Y., Chiamprasert, S., Hsu, Y. Z. and Perera, F. P. (1998) Associations between both genetic and environmental biomarkers and lung cancer: evidence of a greater risk of lung cancer in women smokers. *Carcinogenesis*, **19**, 1949–1953.
13. Brody, J. G., Moysich, K. B., Humblet, O., Attfield, K. R., Beehler, G. P. and Rudel, R. A. (2007) Environmental pollutants and breast cancer: epidemiologic studies. *Cancer*, **109**, 2667–2711.
14. Steck, S. E., Gaudet, M. M., Eng, S. M., Britton, J. A., Teitelbaum, S. L., Neugut, A. I., Santella, R. M. and Gammon, M. D. (2007) Cooked meat and risk of breast cancer—lifetime versus recent dietary intake. *Epidemiology*, **18**, 373–382.
15. Rundle, A., Tang, D., Hibshoosh, H., Schnabel, F., Kelly, A., Levine, R., Zhou, J., Link, B. and Perera, F. (2002) Molecular epidemiologic studies of polycyclic aromatic hydrocarbon-DNA adducts and breast cancer. *Environ. Mol. Mutagen*., **39**, 201–207.
16. Xiong, P., Bondy, M. L., Li, D., Shen, H., Wang, L. E., Singletary, S. E., Spitz, M. R. and Wei, Q. (2001) Sensitivity to benzo(a)pyrene diol-epoxide associated with risk of breast cancer in young women and modulation by glutathione S-transferase polymorphisms: a case–control study. *Cancer Res*., **61**, 8465–8469.
17. Gammon, M. D., Sagiv, S. K., Eng, S. M., *et al*. (2004) Polycyclic aromatic hydrocarbon-DNA adducts and breast cancer: a pooled analysis. *Arch. Environ. Health*, **59**, 640–649.
18. Guengerich, F. P. (2008) Cytochrome p450 and chemical toxicology. *Chem. Res. Toxicol*., **21**, 70–83.
19. Shimada, T., Gillam, E. M., Oda, Y., Tsumura, F., Sutter, T. R., Guengerich, F. P. and Inoue, K. (1999) Metabolism of benzo[a]pyrene to trans-7,8-dihydroxy-7, 8-dihydrobenzo[a]pyrene by recombinant human cytochrome P450 1B1 and purified liver epoxide hydrolase. *Chem. Res. Toxicol*., **12**, 623–629.
20. Ruan, Q., Gelhaus, S. L., Penning, T. M., Harvey, R. G. and Blair, I. A. (2007) Aldo-keto reductase- and cytochrome P450-dependent formation of benzo[a]pyrene-derived DNA adducts in human bronchoalveolar cells. *Chem. Res. Toxicol*., **20**, 424–431.
21. Joseph, P. and Jaiswal, A. K. (1994) NAD(P)H:quinone oxidoreductase1 (DT diaphorase) specifically prevents the formation of benzo[a]pyrene quinone-DNA adducts generated by cytochrome P4501A1 and P450 reductase. *Proc. Natl. Acad. Sci. U. S. A*., **91**, 8413–8417.
22. Joseph, P. and Jaiswal, A. K. (1998) NAD(P)H:quinone oxidoreductase 1 reduces the mutagenicity of DNA caused by NADPH:P450 reductase-activated metabolites of benzo(a)pyrene quinones. *Br. J. Cancer*, **77**, 709–719.
23. Keshava, C., Divi, R. L., Einem, T. L., Richardson, D. L., Leonard, S. L., Keshava, N., Poirier, M. C. and Weston, A. (2009) Chlorophyllin significantly reduces benzo[a]pyrene-DNA adduct formation and alters cytochrome P450 1A1 and 1B1 expression and EROD activity in normal human mammary epithelial cells. *Environ. Mol. Mutagen*., **50**, 134–144.
24. Keshava, C., Divi, R. L., Whipkey, D. L., Frye, B. L., McCanlies, E., Kuo, M., Poirier, M. C. and Weston, A. (2005) Induction of CYP1A1 and CYP1B1 and formation of carcinogen-DNA adducts in normal human mammary epithelial cells treated with benzo[a]pyrene. *Cancer Lett*., **221**, 213–224.
25. Stampfer, M., Hallowes, R. C. and Hackett, A. J. (1980) Growth of normal human mammary cells in culture. *In Vitro*, **16**, 415–425.
26. Laird, P. W., Zijderveld, A., Linders, K., Rudnicki, M. A., Jaenisch, R. and Berns, A. (1991) Simplified mammalian DNA isolation procedure. *Nucleic Acids Res*., **19**, 4293.
27. Divi, R. L., Beland, F. A., Fu, P. P., *et al*. (2002) Highly sensitive chemiluminescence immunoassay for benzo[a]pyrene-DNA adducts: validation by comparison with other methods, and use in human biomonitoring. *Carcinogenesis*, **23**, 2043–2049.
28. Ciolino, H. P. and Yeh, G. C. (1999) Inhibition of aryl hydrocarbon-induced cytochrome P-450 1A1 enzyme activity and CYP1A1 expression by resveratrol. *Mol. Pharmacol*., **56**, 760–767.
29. Radenac, G., Coteur, G., Danis, B., Dubois, P. and Warnau, M. (2004) Measurement of EROD activity: caution on spectral properties of standards used. *Mar. Biotechnol. (NY)*., **6**, 307–311.
30. Ross, D. and Siegel, D. (2004) NAD(P)H:quinone oxidoreductase 1 (NQO1, DT-diaphorase), functions and pharmacogenetics. *Methods Enzymol*., **382**, 115–144.
31. Shi, Z., Dragin, N., Miller, M. L., *et al*. (2010) Oral benzo[a]pyrene-induced cancer: two distinct types in different target organs depend on the mouse Cyp1 genotype. *Int. J. Cancer*, **127**, 2334–2350.
32. Pratt, M. M., John, K., MacLean, A. B., Afework, S., Phillips, D. H. and Poirier, M. C. (2011) Polycyclic aromatic hydrocarbon (PAH) exposure and DNA adduct semi-quantitation in archived human tissues. *Int. J. Environ. Res. Public Health*, **8**, 2675–2691.
33. Rundle, A., Tang, D., Hibshoosh, H., Estabrook, A., Schnabel, F., Cao, W., Grumet, S. and Perera, F. P. (2000) The relationship between genetic

damage from polycyclic aromatic hydrocarbons in breast tissue and breast cancer. *Carcinogenesis*, **21**, 1281–1289.
34. Kyrtopoulos, S. A. (2006) Biomarkers in environmental carcinogenesis research: striving for a new momentum. *Toxicol. Lett*., **162**, 3–15.
35. Saieva, C., Peluso, M., Masala, G., *et al*. (2011) Bulky DNA adducts and breast cancer risk in the prospective EPIC-Italy study. *Breast Cancer Res. Treat*., **129**, 477–484.
36. Ma, Q. and Lu, A. Y. (2007) CYP1A induction and human risk assessment: an evolving tale of in vitro and in vivo studies. *Drug Metab. Dispos*., **35**, 1009–1016.
37. Uno, S., Dalton, T. P., Dragin, N., Curran, C. P., Derkenne, S., Miller, M. L., Shertzer, H. G., Gonzalez, F. J. and Nebert, D. W. (2006) Oral benzo[a]pyrene in Cyp1 knockout mouse lines: CYP1A1 important in detoxication, CYP1B1 metabolism required for immune damage independent of total-body burden and clearance rate. *Mol. Pharmacol*., **69**, 1103–1114.
38. Arlt, V. M., Poirier, M. C., Sykes, S. E., John, K., Moserova, M., Stiborova, M., Wolf, C. R., Henderson, C. J. and Phillips, D. H. (2012) Exposure to benzo[a]pyrene of hepatic cytochrome P450 reductase null (HRN) and P450 reductase conditional null (RCN) mice: detection of benzo[a]pyrene diol epoxide-DNA adducts by immunohistochemistry and 32P-postlabelling. *Toxicol. Lett*., **213**, 160–166.
39. Sagredo, C., Øvrebø, S., Haugen, A., Fujii-Kuriyama, Y., Baera, R., Botnen, I. V. and Mollerup, S. (2006) Quantitative analysis of benzo[a]pyrene biotransformation and adduct formation in Ahr knockout mice. *Toxicol. Lett*., **167**, 173–182.